ELSEVIER

Contents lists available at ScienceDirect

Materials Letters

journal homepage: www.elsevier.com/locate/matlet





Multifunctional superelastic graphene aerogels derived from ambient-dried graphene oxide/camphene emulsions

Siyu Tian a, Long Zhou a, Shiwen Wu a, Ruda Jian a, Ashraf Keewan a, Shuang Cui a,b, Guoping Xiong a,*

- a Department of Mechanical Engineering, The University of Texas at Dallas, 800 W Campbell Rd, Richardson, TX 75080, United States
- b National Renewable Energy Laboratory, 15013 Denver W Pkwy, Golden, CO 80401, United States

ARTICLE INFO

Keywords:
Graphene oxides
Camphene
Oil-in-water emulsions
Ambient drying
Graphene aerogels
Multifunctionality

ABSTRACT

Graphene oxide (GO) emulsions have been widely adopted to fabricate lightweight graphene aerogels (GAs). However, preparing high-performance GAs from conventional GO emulsions under ambient conditions seems rather challenging because of the structural collapse caused by strong capillary forces during drying. Here, we report a new, low-cost route to prepare high-performance, multifunctional GAs by the ambient drying of GO/camphene emulsions. Benefiting from the liquid–solid and solid–gas phase transitions of camphene, highly porous GO aerogels were obtained under ambient conditions. Moreover, the thermally annealed GO aerogels exhibited excellent mechanical properties, fire resistance, thermal insulation performance, and oil adsorption capability.

1. Introduction

Three-dimensional (3D) graphene aerogels (GAs) assembled from atomically thin graphene sheets have been widely investigated in many applications because of their ultrahigh porosity (> 99 %), outstanding mechanical properties, and excellent thermal performance [1]. Many approaches have been developed to prepare GAs from various precursors, including hydrocarbons (e.g., CH₄), graphene oxide (GO), and exfoliated graphene [1]. Among them, assembling GO sheets into 3D architectures by solution-based techniques such as hydrothermal synthesis [2], freeze-casting [3], and 3D printing [4] are frequently adopted but limited by the drying methods (e.g., lyophilization, supercritical drying). Although sacrificial templates (e.g., polystyrene beads) can be used to fabricate GAs under ambient conditions, the tedious template removal process inevitably introduces contaminants and structural defects into graphene monoliths, resulting in poor structural stability under deformation and high cost for scalable production [5]. Therefore, developing efficient ambient drying approaches is of practical significance to fabricate high-performance and multifunctional GAs.

Emulsion templating based on two immiscible liquids has become a promising method for preparing graphene-based monoliths [6]. However, obtaining porous graphene structures via subsequent ambient drying of GO emulsions remains challenging. Here, we highlight the

facile fabrication of GAs based on the ambient drying of GO/camphene emulsions. After the complete solvent removal and a subsequent reduction of GO aerogels, high-performance and multifunctional GAs were obtained. The GAs exhibited ultralow density (1.37 mg/cm³), excellent compressibility (> 99%), high oil absorptivity, and outstanding thermal insulation performance. This work provides a feasible, cost-effective strategy for the scalable production of high-performance, multifunctional GAs and may offer new opportunities to fabricate other 2D-material aerogels.

2. Experimental

2.1. Preparation of GAs

GO was prepared using a modified Hummers' method according to the procedures described in our prior work [7]. A mixture of camphene (20 mL) and GO solutions (20 mL, 5–25 mg/mL) was heated in a water bath kept at 80°C. Then, sodium dodecyl sulfate solutions (0.5 mL, 250 mg/mL) were added to the mixtures, followed by mechanical shaking to form homogeneous GO/camphene emulsions. The GO/camphene emulsions were casted on Teflon films using a doctoral blade moving at 5 mm/s and dried under ambient conditions (25°C, 1 atm, 50% RH) to obtain GO aerogels. A dry chamber (Fig. S1) was designed to study the

E-mail address: guoping.xiong@utdallas.edu (G. Xiong).

^{*} Corresponding author.

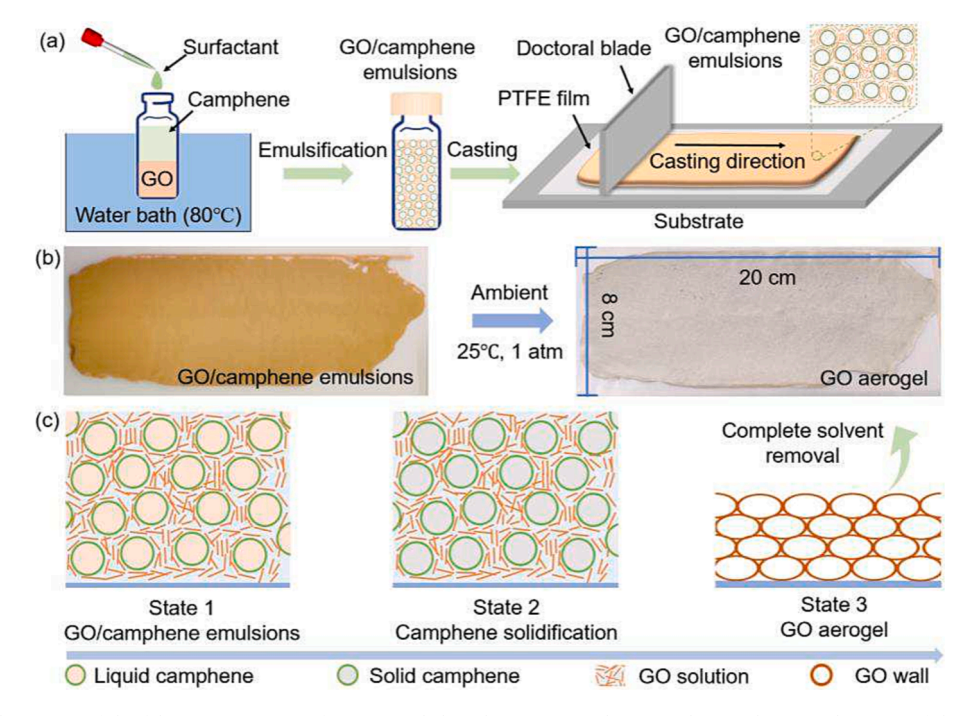


Fig. 1. (a) Schematic illustration of the fabrication process of GO aerogels based on GO/camphene emulsions. (b) Optical images of the casted and ambient-dried GO/camphene emulsions. (c) Schematic illustration of the ambient drying mechanisms of GO/camphene emulsions.

influence of surrounding humidity on the drying of GO/camphene emulsions. Finally, GO aerogels were thermally annealed at $1,000^{\circ}$ C for 2 h in argon to prepare high-performance GAs. The as-obtained GAs were cut into specific shapes using a laser cutter (VLS3.60DT, ULS) for further tests.

2.2. Characterization

The liquid structures and ambient drying process of the GO/camphene emulsions were studied under an optical microscope (OM, AmScope B120). The pore structures of GAs were characterized by a field-emission scanning electron microscope (SEM, Supra 40, Zeiss). The mechanical tests were conducted on a universal testing machine (Instron

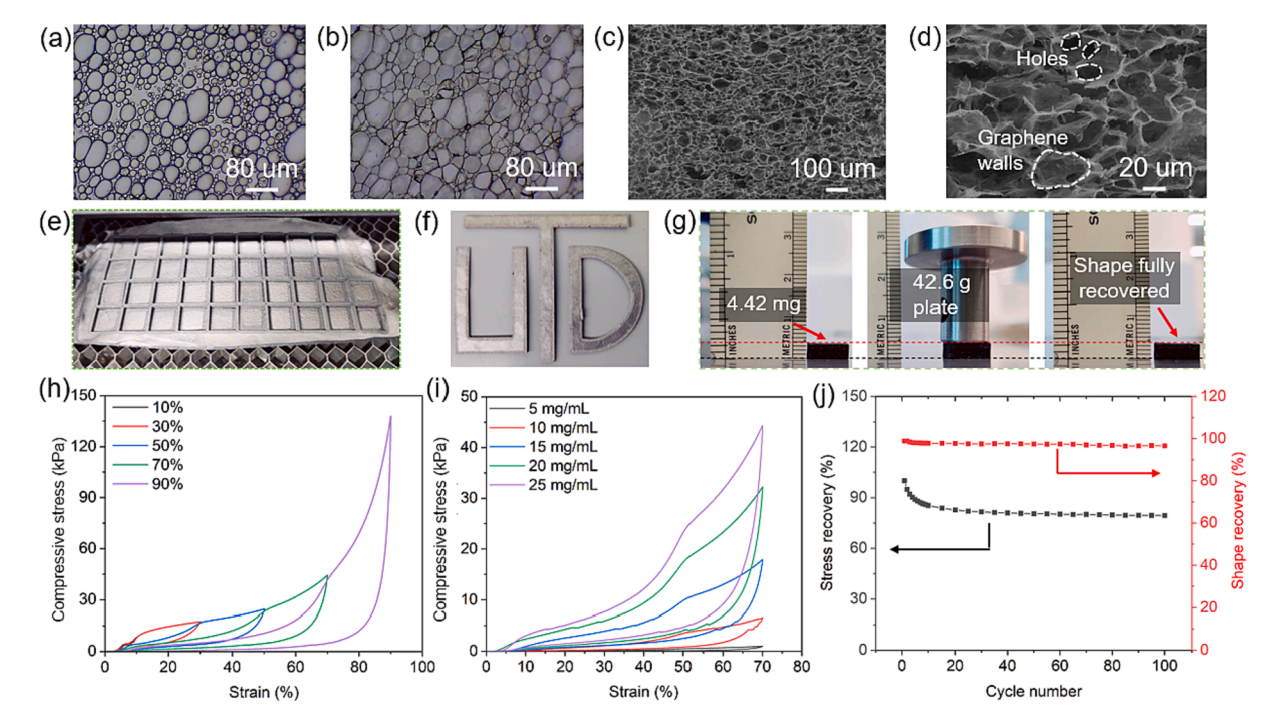


Fig. 2. Optical images of the GO/camphene emulsion with initial GO concentration of 25 mg/mL at different states: (a) State 1 – melted camphene encapsulated by GO solutions, (b) State 2 – solidified camphene encapsulated by GO solutions. (c) and (d) Cross-sectional SEM images of the GAs derived from GO/camphene emulsions. (e) and (f) Optical images of the GAs designed by laser cutting. (g) Optical images showing that the GA (1×1 cm², 4.42 mg) can support a stainless steel plate (42.6 g), and its shape can fully recover from 99% strain. (h) Stress-strain curves of a GA at different compressive strains. (i) Comparative stress-strain curves of GAs derived from different GO concentrations. (j) Mechanical stability of GA over 100 loading-unloading cycles.

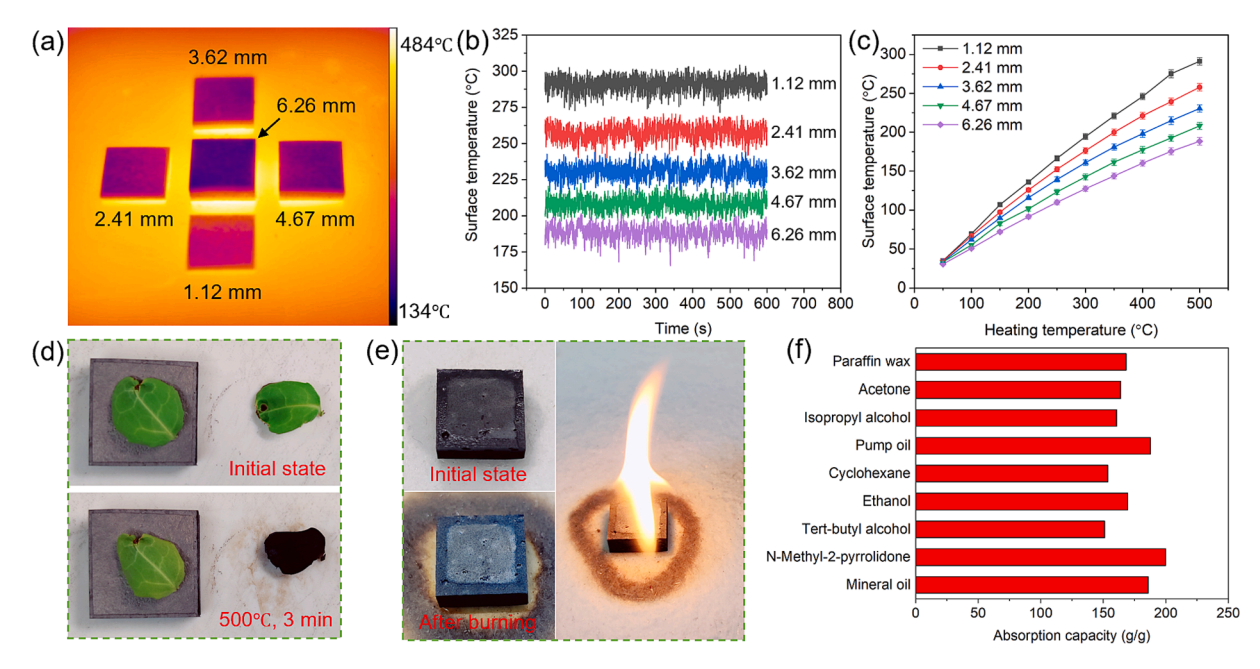


Fig. 3. (a) IR image of the GAs with different thicknesses heated at 500° C. (b) Surface temperatures of GAs recorded by the software (ResearchIR, FLIR). (c) Average surface temperatures of the GAs in the heating temperature range of $50 - 500^{\circ}$ C. (d) Optical images demonstrating the excellent thermal insulation performance of GAs. (e) Optical images showing a GA fully absorbed with mineral oil and after burning out the mineral oil, demonstrating the excellent fire resistance of GAs. (f) Oil adsorption capacities of GAs.

5567). The contact angle test was performed on a goniometer (Kruss DSA 100). The thermal images of GAs were recorded by an infrared (IR) camera (A655sc, FLIR) to investigate the thermal insulation performance. The thermal conductivity was measured at room temperature in air by a trident thermal conductivity instrument with a modified transient plane source. The separation of oil-in-water emulsions was conducted on a homemade filtration device (Fig. S2) using GA as filtration membrane.

3. Results and discussion

Fig. 1a schematically illustrates the fabrication of GO aerogels. The GO/camphene emulsions became viscous at high GO concentrations (> 15 mg/mL, Fig. S3) once cooled down to room temperature. The viscous GO/camphene emulsions with a thickness of 2 mm were tape-casted and ambient-dried for 2 days to obtain GO aerogels (8 \times 20 cm², Fig. 1b). The height of GO aerogels was proportional to the thickness of casted GO/camphene emulsions (Fig. S4). Because of the appropriate melting/ freezing temperature (\sim 50°C) and high vapor pressure (0.4 kPa at 20°C) of camphene, the encapsulated camphene underwent liquid-solid (solidification, state $1 \rightarrow$ state 2) and subsequent solid–gas (sublimation, state $2 \rightarrow$ state 3) phase transitions during ambient drying, as illustrated in Fig. 1c. The solidified camphene acted as supporting cores and rigid templates for GO walls and outbalanced the capillary force induced by water evaporation, thus efficiently preventing the structural collapse and cracking of GO aerogels. Additionally, the solid-gas phase transition of camphene was free of capillary force and ensured its complete removal under ambient conditions without post-processing and residual contaminants. Compared with the prevalent freeze-drying method, the ambient drying of GO/camphene emulsions can provide a low-cost and scalable process for constructing graphene-based aerogels.

At the initial state (Fig. 1c and Fig. 2a), melted camphene was well-encapsulated by GO solutions, forming spherical camphene-in-GO droplets. Once cooled to room temperature, the encapsulated camphene turned into solid-state crystals (Fig. 2b and Fig. S5). The compact graphene walls of thermally annealed GO aerogels exhibited a well-defined cellular-like structure with the cell dimension ranging from $12 \text{ to } 100 \,\mu\text{m}$ (Fig. 2c and d), agreeing well with the droplet sizes of GO/

camphene emulsions (Fig. 2a). The density of GAs was tuned from 1.37 to 9.94 mg/cm³ by varying the initial GO concentration from 5 to 25 mg/mL (Fig. S6). Meanwhile, the GAs with different densities possessed a similar pore structure (Fig. S7). For GO/camphene emulsions dried under low-humidity conditions (25°C, 1 atm, 16% RH), the prepared GAs exhibited a similar pore structure (Fig. S8) compared to that of the GAs dried under normal ambient conditions (25°C, 1 atm, 50% RH).

Fig. 2e and f display the optical images of the GAs in different shapes (e.g., 1×1 cm² squares, UTD letters) designed by laser cutting. GA blocks with well-defined dimensions were patterned in a relatively large scale (e.g., 38 pieces, Fig. 2e) from thermally annealed GO aerogels. More importantly, the as-obtained GAs exhibited excellent mechanical properties. As illustrated in Fig. 2g, a typical GA $(1 \times 1 \text{ cm}^2, 4.42 \text{ mg})$ can support > 9,600 times of its own weight (equivalent to a compressive stress of 4.35 kPa) without noticeable deformations, and its shape can recover from 99% of the strain. Fig. 2h presents the stress-strain curves of the GA (9.94 mg/cm³) at different strain levels. The GA showed maximum stresses of 8.41 and 137.97 kPa at 10% and 90% compressive strains, respectively. At a compressive strain of 70%, the maximum compressive stress of GAs monotonously increased from 0.55 to 24.69 kPa when the density of GAs increased from 1.37 to 9.94 mg/ cm³ (Fig. 2i and Fig. S9), corresponding to high stress/density ratios up to 2,480 Pa/(mg/cm³), which are significantly higher than those of the GAs reported in prior work (e.g., 1,551 Pa/(mg/cm³)) [8]. Furthermore, the GAs exhibited excellent stress and shape recoveries over 100 compression cycles (Fig. 2j and Fig. S10). The height of the GA remained nearly the same as that at the initial state, and the maximum stress retained 80% of its initial value after 100 compression cycles, outperforming those of freeze-casted [8] and 3D-printed [4] GAs. The maximum stresses decreased by 17.3% in the first 20 cycles and then by only 3.3% in the following 80 loading-unloading loops, signifying the excellent long-term mechanical stability of the GAs.

Fig. 3 shows the outstanding thermal insulation performance, fire resistance, and oil adsorption capability of the GAs. When heated on a hot plate kept at 500°C, the surface temperatures decreased with the increasing thickness of GAs (Fig. 3a and b). The surface temperatures of the GAs were recorded for 10 min (Fig. 3b) at equilibrium to calculate their average values. As shown in Fig. 3c, the GA with a thickness of

6.26 mm displayed a surface temperature of 188°C when heated at 500°C because of its ultralow thermal conductivity of 15 ± 0.27 mW/ (m·K), significantly lower than that of the GAs prepared in our prior work [9] and further confirming its excellent thermal insulation performance. These results demonstrated that GAs with ultralow densities and cellular-like structures can effectively block the strong heat convection, conduction, and radiation in air, thus effectively isolating the heat and protecting other materials from high-temperature damages. Consequently, a green leaf placed on the GA remained intact for 3 min at 500°C (Fig. 3d). Moreover, the GAs exhibited outstanding fire resistance (Fig. 3e), superoleophilicity (Fig. S11), and excellent oil adsorption performance (Fig. 3f and Table. S1, see details in SI).

4. Conclusions

In summary, we present a facile, cost-effective route to fabricate lightweight, multifunctional graphene-based aerogels by drying GO/camphene emulsions under ambient conditions. The phase transitions of the encapsulated camphene significantly determine the formation of porous graphene-based architectures. The dispersed camphene droplets in GO/camphene emulsions not only serve as the template for the formation of pore structures but also prevent their structural collapse during ambient drying. The thermally annealed GAs exhibit excellent mechanical/thermal properties and high oil adsorption capability, making them promising for many applications such as strain sensing, thermal insulation, solar-thermal vapor generation, and oil recovery. This ambient drying process may also facilitate fabricating highly porous architectures based on other advanced nanomaterials.

CRediT authorship contribution statement

Siyu Tian: Conceptualization, Methodology, Investigation, Writing – original draft. **Long Zhou:** Investigation, Validation. **Shiwen Wu:** Formal analysis, Writing – review & editing. **Ruda Jian:** Formal

analysis. **Ashraf Keewan:** Investigation. **Shuang Cui:** Investigation. **Guoping Xiong:** Funding acquisition, Supervision, Conceptualization, Writing – review & editing.

Declaration of Competing Interest

The authors declare that they have no known competing financial interests or personal relationships that could have appeared to influence the work reported in this paper.

Data availability

Data will be made available on request.

Acknowledgements

G.X. thanks the University of Texas at Dallas startup fund and the support from the NSF (Grant Nos. CMMI-1923033, CBET-1949962 and CBET-1937949).

Appendix A. Supplementary data

Supplementary data to this article can be found online at $\frac{https:}{doi.}$ org/10.1016/j.matlet.2022.133128.

References

- [1] Z. Sun, et al., Chem. Rev. 120 (18) (2020) 10336-10453.
- [2] Y. Xu, et al., ACS Nano 4 (7) (2010) 4324-4330.
- [3] H.-L. Gao, et al., Nat. Commun. 7 (1) (2016) 12920.
- [4] C. Zhu, et al., Nat. Commun. 6 (1) (2015) 6962.
- [5] Q. Han, et al., Carbon 122 (2017) 556–563.
- [6] Y. Li, et al., Adv. Mater. 26 (28) (2014) 4789-4793.
- [7] M. Sakhakarmy, et al., Int. J. Adv. Manuf. Technol. 114 (1) (2021) 343-355.
- [8] M. Yang, et al., ACS Nano 11 (7) (2017) 6817-6824.
- [9] Q. Zhang, et al., ACS Appl. Mater. Interfaces 9 (16) (2017) 14232–14241.